QUASI-STATIONARY SOLAR WIND IN RAY STRUCTURES OF THE STREAMER BELT

V. G. ESELEVICH and M. V. ESELEVICH
Institute of Solar-Terrestrial Physics, Irkutsk, Russia (e-mail: esel@iszf.irk.ru)

(Received 28 February 2000; accepted 14 April 2000)

Abstract. It is shown on the basis of analyzing the LASCO/SOHO data that the main quasi-stationary solar wind (SW), with a typical lifetime of up to 10 days, flows in the rays of the streamer belt. Depending on R, its velocity increases gradually from $V \approx 3$ km s^{-1} at $R \approx 1.3\ R_\odot$ to $V \approx 170$ km s^{-1} at $R \approx 15\ R_\odot$. We have detected and investigated the movement of the leading edge of the main solar wind at the stage when it occupied the ray, i.e., at the formative stage of a quasi-stationary plasma flow in the ray. It is shown that the width of the leading edge of the main SW increases almost linearly with its distance from the Sun. It is further shown that the initial velocity of the inhomogeneities ('blobs') that travel in the streamer belt rays increases with the distance from the Sun at which they originate, and is approximately equal to the velocity of the main solar wind which carries them away. The characteristic width of the leading edge of the 'blob' $\delta \approx R_\odot$, and remains almost unchanging as it moves away from the Sun. Estimates indicate that the main SW in the brightest rays of the streamer belt to within distances at least of order $R \approx 3\ R_\odot$ represents a flow of collisional magnetized plasma along a radial magnetic field.

1. Introduction

Characteristics of solar wind (SW) flows in the streamer belt are distinguished in the observed complex structure of the white-light corona. According to Eselevich and Eselevich (1999; subsequently referred to as Paper I) who used the LASCO C2 and C3 data, the streamer belt is a sequence of radial rays of increased brightness. A minimum angular size of a single ray $d \approx 2^\circ$–3°, and its lifetime can be as long as 10 days. Inside the rays there randomly arise anti-sunward moving inhomogeneities of material with a typical lifetime of about several hours which were given the name 'blobs' (Sheeley *et al.*, 1997; Wang *et al.*, 1998). The above considerations suggest that both the main quasi-stationary solar wind whose characteristics vary relatively slowly with time, and sporadic wind flows with typical lifetimes of about a few hours or shorter appear to exist in the streamer belt in the absence of CMEs. The latter type should also include the recently discovered sporadic plasma flows, both anti-sunward and sunward, which are produced when the streamer decays, presumably as a consequence of the process of magnetic field line reconnection (Wang *et al.*, 1999a; Wang *et al.*, 1999b). The objective of this paper is to investigate the characteristics of the main quasi-stationary solar wind flowing in ray structures of the streamer belt.

Solar Physics **195:** 319–332, 2000.

2. Data of Analysis

This study is based on using the data on the white-light corona from the LASCO C2 and C3 instruments on the SOHO spacecraft available via the Internet. The C2 coronograph produces images of the white-light corona within 2–6 $R_\odot$. Daily images in MPEG format were used. The time interval between adjacent frames did not exceed one hour, on average. Selected data for the years 1996, 1997 and 1998 were used in the analysis. To minimize the possible influence of the features of the data analyzed we have adhered to the following principles:

(1) Only bright ray structures (whose brightness markedly exceeded the surrounding background brightness) within $R = 2–20\ R_\odot$ from the Sun's centre were investigated.

(2) Emphasis in our study was placed not on absolute brightness distributions of the corona but on their relative variations with time. Also, the time interval in each case under investigation did not exceed several days. This permitted us to eliminate the influence of possible gradual changes in instrument performance in the course of time.

(3) We studied radial structures in the corona, with the projection Λ of their latitude onto the plane of the sky not exceeding $\pm 30°$. The count of Λ is positive northward of the equator and negative southward.

3. Identification and Properties of an Isolated Ray – the Velocity of a Quasi-Stationary Solar Wind in the Ray

A narrow ray ($d \approx 2°–3°$) of the streamer belt, with no other rays (or no other structures with increased brightness) on either side of which strictly along the parallel at distances $\leq \pm 35°$, will be referred to as isolated. Let such a ray, co-rotating with the Sun, intersect the plane of the sky. Because of the property of the Thomson scattering of photospheric emission from electrons of the corona, the ray when observed on the limb will be recorded in the direction of solar rotation as a broad one, with a typical angular size of $\approx 70°$ (Hundhausen, 1993). The projection of its latitude Λ on the plane of the sky will vary with time, and the character of this variation depends on the latitude of the ray λ on the Sun, and on the heliographic latitude of the Sun's disk centre B_0. Therefore, on the synoptic chart the ray will describe a certain curve which is defined by formula (6) in the Appendix of Paper I.

There are two possibilities of observing and investigating an isolated ray of the streamer belt as it passes the plane of the sky: in the first place, when the ray lies in the portion of the belt that is elongated along the meridian (this case was analyzed in detail in Paper I); and, secondly, when the ray is at the point of curvature of the belt which is at a maximum distance northward or southward of the solar equator. This can be seen on synoptic charts of white-light corona brightness (constructed

using the data from the LASCO C2 instrument on the SOHO spacecraft and available via the Internet) as separate segments of thin white arcs, with their bulges normally facing the equator. For example: CR 1910, E-limb, arc at $\approx 7^\circ - 10^\circ$ N, 2–8 November 1996; CR 1911, E-limb, arch at $\approx 12^\circ - 17^\circ$ N, 29 June–4 July 1996; CR 1996, E-limb, arch at $\approx 20^\circ - 30^\circ$ N, 23–29 August 1996; CR 1914, E-limb, arch at $\approx 32^\circ - 38^\circ$ N, 19–23 September 1996; CR 1915, W-limb, arch at $\approx 20^\circ - 30^\circ$ S, 25 October–31 November 1996, etc. The agreement between the observed position and the form of the ray's arch on the synoptic chart and calculated ones permits a reasonably reliable identification of the isolated ray (as was demonstrated in Paper I).

The technique for extracting experimental information from the white-light corona image involved the following consecutive procedures.

For each of the images from daily MPEG files, brightness distributions, P, of the corona were constructed depending on the angle Λ at different distances R from the Sun's centre, separately for E limb and W limb. After that, the ray brightness P_R was inferred (its definition may be found in Paper I).

The possibility of introducing the notion of the ray brightness P_R is dictated by the fact that the ray is distinguished on the brightness profile P by the steepness of the slope of its two forming lines which can be represented by straight lines from the top of P_M (maximum brightness of the ray) to the inflection points A and B. This permits us to introduce a definition of the ray brightness P_R and of the angular size d, such as shown in the upper panels of Figures 1 and 2 from Paper I. To separate the ray from the remaining part of the signal and hence of determining the ray brightness P_R and the angular size d, the following procedure was used: a smoother curve P_S was found for each profile P by averaging the curve P over the angle of $6^\circ - 7^\circ$. Next, this averaged curve was subtracted from the original profile P and the brightnesses of individual rays were determined using the relation: $P_R = P_M - P_S$.

Based on the ideology introduced above, we now compare the observational data for isolated rays with calculations by considering an example of two events: 2–9 June 1996, E limb, latitude $\lambda \approx 7^\circ$ N, and 29–31 October 1996, W limb, latitude $\lambda \approx 20^\circ$ N. Dark circles in the upper panels of Figures 1 and 2 show experimental positions of brightness maxima of rays P_M (or the ray brightness P_R) at consecutive points in time, respectively, at $R = 4.5\ R_\odot$ for 2–9 June 1996 (E limb), and at $R = 4.0\ R_\odot$ for 29–31 October 1996 (W limb). The lower abscissa axis indicates the time of observation on W or E limb, and the upper abscissa axis indicates the deviation $\delta\psi_L$ of the ray from the plane of the sky.

A family of calculated curves for latitudes λ near, the observed rays, respectively, for $B_\circ = 0.5^\circ$ (Figure 1) and 4.7° (Figure 2), is shown by dashed curves. The observed curves agree nicely with the calculated ones for $\lambda \approx 7^\circ$ (Figure 1, top) and $\lambda \approx 19.5^\circ$ (Figure 2, top) (maximum deviations on most of the curves do not exceed $\pm 0.5^\circ$, and only at the ends of the curve in Figure 1 where the ray brightness P_R becomes small, it reaches $\pm 1.0^\circ$). Experimental time dependencies

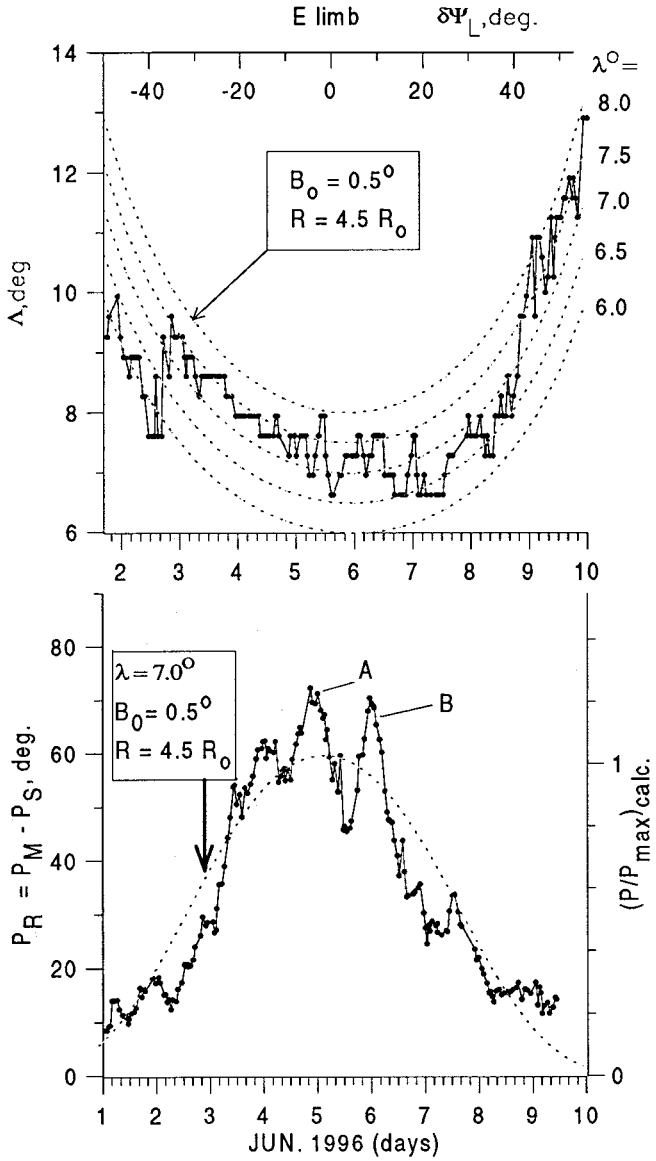

Figure 1. Isolated ray of the streamer belt, lying at the farthest (from the solar equator) bend point at the northern latitude $\lambda \approx 7°$ when this ray transited the plane of the sky on E limb on 5 June 1996 (the time is indicated on the lower abscissa axis). *Top: dark circles* – dependence of the projection of the latitude Λ onto the plane of the sky of the observed positions of the ray brightness P_R on the angular deviation $\delta\psi_L$ of the ray under consideration with respect to the plane of the sky; *dotted curves* – calculated curves, similar to the observed curve, for $\lambda = 6.0, 6.5, 7.0, 7.5, 8.0$ deg. *Bottom: dark circles* – observed time dependence of the value of the ray brightness P_R; *dotted curve* – calculated curve (right vertical axis in relative units), similar to the observed time dependence, for the value of $\lambda = 7.0°$. $B_\circ = 0.5°$, $R = 4.5\ R_\odot$.

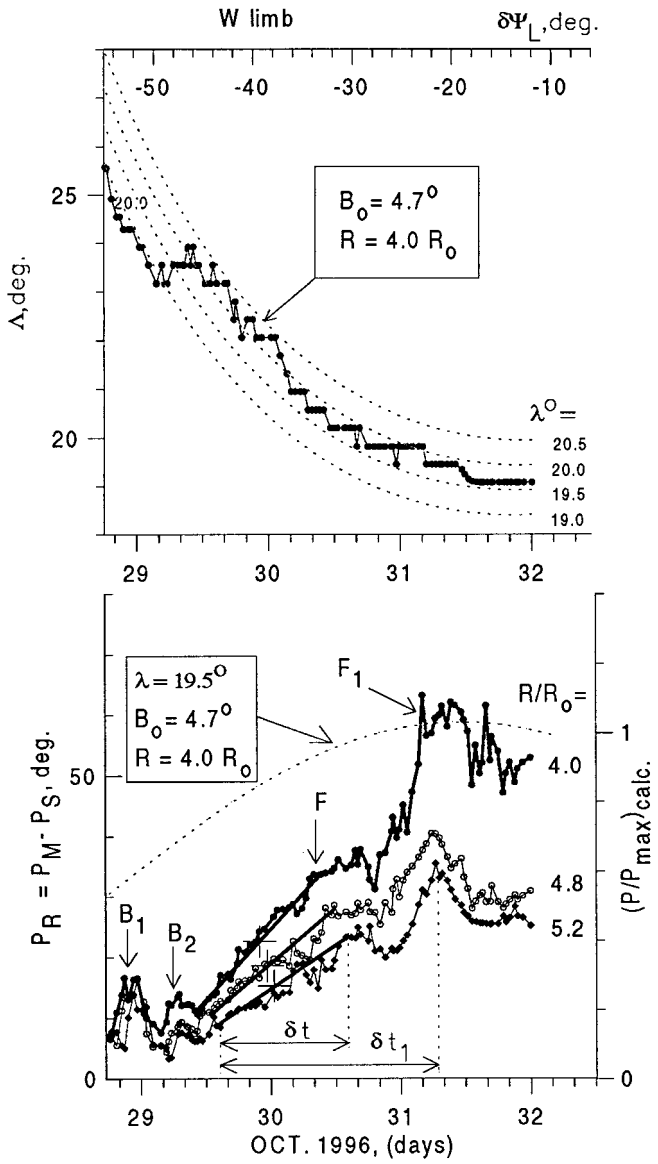

Figure 2. Isolated ray of the streamer belt, lying at the farthest (from the solar equator) bend point at the northern latitude $\lambda \approx 20^\circ$ when this ray transited the plane of the sky on E limb on 31 October 1996 (the time is indicated on the lower abscissa axis). *Top: dark circles* – dependence of the projection of the latitude Λ onto the plane of the sky of the observed positions of the ray brightness P_R on the angular deviation $\delta\psi_L$ of the ray under consideration with respect to the plane of the sky; *dotted curves* – calculated curves, similar to the observed curve, for $\lambda = 19.0$, 19.5, 20.0, and 20.5 deg. *Bottom: dark circles* – observed time dependence of the value of the ray brightness P_R; *dotted curve* – calculated curve, (right vertical axis in arbitrary units), similar to the observed time dependence, for the value of $\lambda = 19.5^\circ$. $B_\circ = 4.7^\circ$, $R = 4.0\ R_\odot$.

of the value of ray brightness P_R for each of these rays are shown in the lower panels of Figures 1 and 2 by dark circles, and the calculated curves similar to them appear as dashes.

For the ray in Figure 1 (bottom), the oscillation-averaged profile of the observed distribution $P_R(t)$ is in reasonably good agreement with the calculated curve. This means that this ray involves a predominant quasi-stationary solar wind flow (the oscillation-averaged SW plasma density changes relatively little during 9 days as a minimum and is therefore similar to the calculated dependence). The plasma brightness (density) jumps, superimposed on the averaged curve, correspond to the inhomogeneities (or 'blobs') which travel with the velocity of the main SW. In Figure 3, the symbols $*$ ($R = 3.7\ R_\odot$) and $\times$ ($R = 3.9\ R_\odot$) show, respectively, the velocities of the inhomogeneity A and B from Figure 1 (bottom) which were determined from the delay time of their appearance at two different distances R_1 and R_2 (the method is described in Paper I, and will be used throughout this paper).

In the case of Figure 2 (bottom), the observed dependence $P_R(t)$ at $R = 4.0\ R_\odot$ (dark dots) differs greatly from the calculated one. The following features are traceable on the experimental curve: 'blobs' B_1 and B_2 are ahead, and they are followed in temporal order by a front of increasing brightness (density) to a maximum value of F_1. Analysis shows that the ensuing behaviour of $P_R(t)$ (after the top of F_1) during two days as a minimum is similar to the calculated one, i.e., starting from the top of F_1 and further as time goes on, a quasi-stationary SW flow is established in the ray. According to Wang *et al.* (1998), the enhancement of the brightness in the 'blob' in comparison with the main solar wind can be as large as 20–30%. This means that the plasma density at the top of the front F_1 in Figure 2 exceeds that at its basis (background plasma) by a factor of two or more. Hence we may deduce that the front of a plasma flow with high plasma density moves into the background plasma of lower density. All this is taking place inside the selected isolated ray.

With distance from the Sun, the temporal width δt_1 (the definition is given in Figure 2 (bottom)) of the front F_1 is increasing progressively, and the front itself is transformed, breaking down into separate areas of inhomogeneities which subsequently either merge with other areas or turn into 'blobs'. Nevertheless, on some segments of the path at the radial distance, it is always possible to measure the velocity of the midpoint of the entire front or of some part of it. In Figure 2 (bottom), the midpoint of a portion of the front with its top at the point F is shown by a cross (the averaging over the oscillations of the front is shown by straight lines), and the temporal width of the front is designated by δt. The dependence of the velocity $V(R)$ for this point is shown in Figure 3 by dark circles. The front width $\delta(R) \approx \delta t V(R)$ increases almost linearly with increasing R (solid line F with dark circles in Figure 4).

It is evident from the dependence $V(R)$ for 'blob' B_1 (dashed curve B_1 with triangles in Figure 3) that within $R = 2.6$–$3.2\ R_\odot$ the 'blob' travels with about the main SW velocity, i.e., in about the same manner as do the small inhomogeneities 1 and 2 in the event of 4–6 June 1996 in Figure 1 (their velocities in Figure 3 are

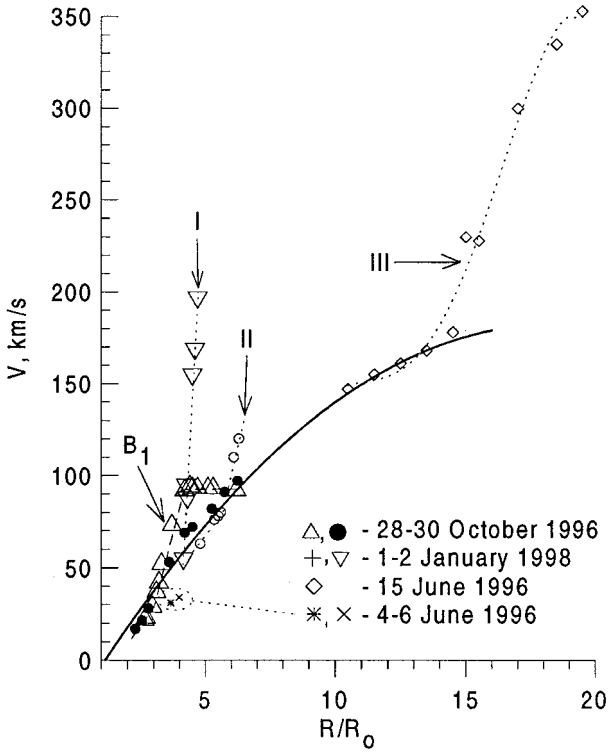

Figure 3. Velocity dependencies $V(R)$ of the following features travelling inside the rays: (a) Fronts of inhomogeneity ('blob') ∇, $\circ$ – on W limb ($\lambda = -14°$) on 2 January 1998 (*dotted lines* I and II), $\triangle$ – on W limb ($\lambda = 23°$) on 28–29 October 1996 (*dashed line* B_1), $\diamond$ – on E limb ($\lambda = 1°$) on 15 June 1996, (*dotted line* III), $*$ and $\times$ – fronts of inhomogeneities ('blobs') A (at $R = 3.7\ R_\odot$) and B ($R = 3.9\ R_\odot$), respectively, on E limb ($\lambda \approx 7°$) on 4–6 June in Figure 1 (bottom). (b) $\bullet$ – front of a high-density plasma flow into a lower-density background plasma, ($\lambda \approx 23°$), E limb, 29–30 October 1996. The solid curve corresponds to the initial minimum velocities of the fronts of the inhomogeneities ('blobs') that are produced at different R.

shown, respectively, by the symbols $*$ ($R = 3.7\ R_\odot$) and $\times$ ($R = 3.9\ R_\odot$). Within $R = 3.2$–$4.4\ R_\odot$, an abrupt acceleration of the inhomogeneity under the action of some unknown mechanism is observed (i.e., it turns into a 'blob'); subsequently, within $R > 4.4\ R_\odot$, it is decelerated with respect to the main SW; after that, the velocity equals that of the main wind.

The 'blob's' front width δ, unlike the front F of plasma flow, remains almost unchanged as the 'blobs' move away from the Sun (dashed line B_1 in Figure 4). A possible explanation for this difference is as follows. The front F of high-density plasma moves and broadens into the background plasma along the radius. Therefore, the magnetic field (which is also directed along the radius) does not affect these processes. A similar spreading process of the flow forefront was investigated by Zeldovich and Raizer (1966) in the case of the expansion of the gas into a

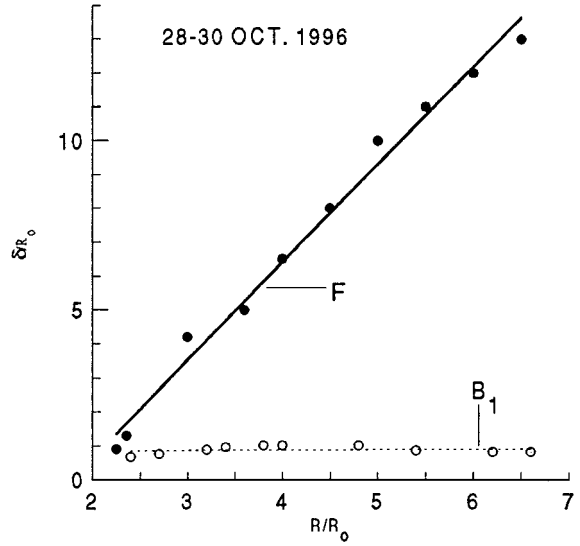

Figure 4. $R/R_{\odot}$-dependencies of the normalized front width: B_1 – 'blob', F – high-density plasma flow moving into the lower-density background plasma inside the ray with $\lambda \approx 20^{\circ}$ on E limb on 28 –30 October 1996.

vacuum. It was shown that in this case the typical spreading velocity of the front is the sound velocity. Knowing the value of the broadening of the front $(\delta_2 - \delta_1)$ with distance R, it is possible to estimate the sound velocity $V_S = (\gamma(T_e + T_p)/m_p)^{1/2}$ from the relation

$$V_S \sim \frac{(\delta_2 - \delta_1)(V_2 + V_1)}{4(R_2 - R_1)}\,, \tag{1}$$

where δ_2, V_2 and δ_1, V_1 are the width and velocity of the front F of plasma flow at distances R_2 and R_1, respectively; T_e and T_p are, respectively, the electron and proton temperatures; $\gamma = \frac{5}{3}$ is the adiabatic exponent. $T(R) = (T_e + T_p)/2$ was estimated by formula (1) at $\approx (4\text{–}5) \times 10^5$ K at $R = 5\text{–}6\ R_{\odot}$.

In the case of the 'blob', however, it has its own transverse (with respect to the radial direction) magnetic fields which keep the front from spreading.

In our recent paper (Eselevich and Eselevich, 2000) we have shown that the initial velocity of the 'blob' increases with distance from the Sun, at which it is produced, and is about the velocity of the main solar wind which carries it away. The solid curve in Figure 3 corresponds to the initial minimum velocities of different 'blobs' (or the initial portion of the velocity profile with a minimum slope) at different R in the rays which were observed on: (∇, $\circ$) – W limb ($\lambda = -14^{\circ}$) on 2 January 1998 (dashed lines I and II), ($\triangle$) – W limb ($\lambda = 23^{\circ}$) on 28–29 October 1996 (dashed line B_1), and ($\diamond$) – E limb ($\lambda = 1^{\circ}$) on 15 June 1996, (dashed lines III). The proximity of this curve and the dark dots in Figure 3 does imply an agreement between the two independent methods of measuring the dependence

$V(R)$ of the main solar wind: from the velocity of the front F of the main SW when it occupies the ray (or at the stage of formation of a quasi-stationary plasma flow inside the ray), and from the velocity, with which the brightness (density) inhomogeneities are carried away by the main quasi-stationary SW.

4. The Quasi-Stationary Solar Wind Parameters in the Ray at $R \leq 3\ R_\odot$

4.1. Collisional and magnetic character of solar wind plasma in the ray

We now seek to estimate the parameters of a quasi-stationary SW that travels inside an arbitrary ray structure of the streamer belt. As is evident from the above discussion, such a SW is a plasma flow along a radially directed magnetic field. Of fundamental importance is the question of the role played by Coulomb collisions in plasma flow of this kind. The role of the collisions is decisive, and the plasma is considered collisional in relation to the processes of our interest if the following conditions are satisfied:

$$l, \delta \gg \lambda_e, \lambda_p, \qquad \tau_{en} \ll l/V\ , \tag{2}$$

where l is a typical scale of decrease in SW plasma density as a function of R (the distance, at which the density decreases by a factor of e); δ is the forefront width of the SW quasi-stationary stream; and λ_e and λ_p, respectively, are the free path lengths with respect to electron-electron (electron−proton) and proton−proton collisions; τ_{en} is the time of energy exchange between electrons and ions, and V is the SW velocity.

Let us estimate the conditions (2) for particle collisions in the ray of increased brightness in the streamer belt within distances $\leq 3\ R_\odot$. For this purpose, the plasma parameters at $R \approx 3\ R_\odot$ needed to make this estimate will be based on the following data and reasoning.

(A) With increasing R, the electron temperature T_e in the streamer belt, according to the recent data from the SOHO spacecraft (David *et al.*, 1997), decreases from $\approx 1.2 \times 10^6$ K at $R \approx 1.02\ R_\odot$ to $\approx 0.8 \times 10^6$ K at $R \approx 1.4\ R_\odot$. With such a decrease in electron temperature with distance, one might expect $T_e < 10^6$ K for $R \approx 3\ R_\odot$, at least.

(B) According to Dollfus and Martres (1977) the plasma density n in separate rays of the streamer belt can range from $\approx 10^6$ cm^{-3} to $\approx 7 \times 10^6$ cm^{-3} at $R \approx 3\ R_\odot$. For our estimate, we take $n \approx 3.5 \times 10^6$ cm^{-3}, and the SW velocity $V \approx 40$ km s^{-1}.

For the adopted values n, $T_e \approx T_p \approx 5 \times 10^5$ K, and using the formulas for λ_e and λ_p (Artsimovich, 1961),

$$\lambda_p \approx \frac{2.5 \times 10^4 T_p^2(\mathrm{K})}{n(\mathrm{cm}^{-3}) Z^2}(\mathrm{cm}) \approx \lambda_e \left(\frac{T_e}{T_p}\right)^2 (\mathrm{cm})\ , \tag{3}$$

we find $\lambda_e \approx \lambda_p \leq 0.03\ R_\odot$ (for $Z = 1$, the proton charge).

In this case, at $R \approx 3\ R_\odot$, the value of $\delta \approx 1{-}5\ R_\odot$ (see Figure 4), and $l \approx R_\odot$, i.e., the condition $l, \delta \gg \lambda_e, \lambda_p$ is satisfied.

In the case of protons when $(T_e/m_e)^{1/2} \gg (T_p/m_p)^{1/2}$, from the formula (Artsimovich, 1961)

$$\tau_{en} \approx \frac{17 T_e^{3/2}(\mathrm{K})}{n(\mathrm{cm}^{-3})}(c)\ , \tag{4}$$

we find that $\tau_{en} \approx 1.7 \times 10^3$ s, $l/V \approx 1.8 \times 10^4$ s. That is, the two conditions of (2) are satisfied for the typical scales of all types of plasma flows in the rays under consideration, including 'blobs'. At $R < 3\ R_\odot$, the plasma is all the more collisional because the inequalities (2) are strengthened. When $R > 3\ R_\odot$, the condition $\tau_{en} \ll l/V$ in (2) is no longer satisfied because of the weaker energy exchange between electrons and ions. When $R > 10\ R_\odot$, the condition $l, \delta \gg \lambda_e$, λ_p in (2) is violated, and the SW plasma flow becomes entirely collisionless.

The magnetic field will have a dominating effect on collisional plasma if the magnetization conditions of plasma electrons and ions are satisfied:

$$\rho_e/\lambda_e \ll 1, \quad \rho_p/\lambda_p \ll 1, \tag{5}$$

where

$$\rho_e = \left(\frac{8km_eT_e}{\pi e^2 B^2}\right)^{1/2}, \quad \rho_p = \left(\frac{8km_pT_p}{\pi e^2 B^2}\right)^{1/2} \tag{6}$$

are, respectively, the electron and proton Larmor radii ($k = 1.38 \times 10^{-23}$ J K^{-1}). We infer a magnitude of the magnetic field B at $R \approx 5\ R_\odot$ from the relation

$$B \approx B_e(R_e/R)^2\ , \tag{7}$$

where $R_e = 215\ R_\odot$, and B_e is the typical value of the magnitude of the magnetic field in the solar wind at the Earth's orbit. For $B_e \approx 5 \times 10^{-5}$ G, the value of $B \approx 0.1$ G.

For the above-mentioned plasma parameters and for this value of B, we have $\rho_e/\lambda_e \approx 5 \times 10^{-8}$, $\rho_p/\lambda_p \approx 2 \times 10^{-6}$. Thus the SW plasma is magnetized, virtually all the way from the Sun to the Earth's orbit. An important implication of the analysis made here is the conclusion that the solar wind inside the ray (magnetic tube) represents a collisional plasma flow along the magnetic field at least up to $R \leq 5\ R_\odot$. (Plasma magnetization is important only in the perpendicular direction to the field. The magnetic field does not affect the motion of the plasma along the tube). Such a flow is described by hydrodynamic equations (with no magnetic field) with adiabatic index $\gamma = \frac{5}{3}$. The sound velocity in such a flow is $V_S = (5(T_e + T_p)/3m_p)^{1/2} \approx (10T_e/3m_p)^{1/2}$ (when $T_e \approx T_p$).

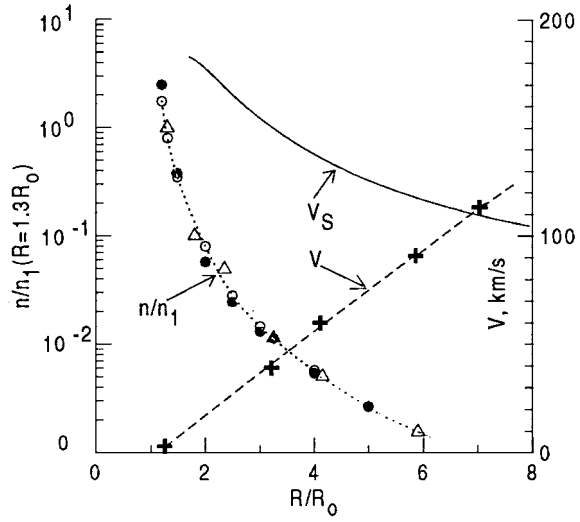

Figure 5. Typical distributions in the increased-brightness ray of the streamer belt depending on $R/R_\odot$: (a) of the measured velocity of the main quasi-stationary flow (+) (a segment of the solid curve from Figure 3 is used), and of the relative plasma density profile n/n_1 (•, ○) from Dollfus and Martres (1977); (b) of the calculated sound velocity V_S (solid line), and of the relative plasma density profile n/n_1 (△).

4.2. R-DEPENDENCE OF THE PLASMA DENSITY $n(R)$, SOUND VELOCITY $V_S(R)$, AND TYPICAL PLASMA TEMPERATURE $T(R) = [T_e(R) + T_p(R)]/2$ IN THE RAY OF THE STREAMER BELT

Knowing the dependence $V(R)$ of a quasi-stationary plasma flow along a radial ray, it is possible to calculate the distributions of the density $n(R)$, sound velocity $V_S(R)$ and temperature $T(R) = [T_e(R) + T_p(R)]/2$ of the flow plasma, and to compare them with the observed distributions. From the law of conservation of flow along a radially expanding magnetic tube, we have

$$\frac{n}{n_1} = \left(\frac{R_1}{R}\right)^2 \left(\frac{V_1}{V}\right) , \tag{8}$$

where V_1 is the known value of the flow velocity at the distance R_1 nearest to the Sun. In the this case $V_1 \approx 3$ km s^{-1} at $R_1 \approx 1.3\ R_\odot$. The variation of the main quasi-stationary SW, $V(R)$, in the ray which was used to construct the dependence $n(R)/n_1$ (open triangles in Figure 5), for $R \approx (1.3–6.0)\ R_\odot$, is shown in Figure 5 by hatching and crosses (this is the left-hand half of the solid curve in Figure 3).

The resulting distribution $n(R)/n_1$ is in reasonably good agreement with the relative density behaviour for two separate rays measured by Dollfus and Martres (1977) on 15 February 1961 solar eclipse (dark and open circles in Figure 5).

Knowing the experimental variation $V(R)$ for a radial plasma flow in the ray, it is possible to calculate, within the hydrodynamic approximation, the dependencies

$V_S(R)$ and $T(R) = [T_e(R) + T_p(R)]/2$. In the case of $\gamma = 1$ and $T_e \approx T_p$, the equation governing the relation between $V_S(R) = [2(T_e/m_p)]^{1/2}$ and $V(R)$ is given by formula (8) from Sheeley *et al.* (1997). For $\gamma > 1$ this equation has the form:

$$\frac{V_S^2(R)}{VR^2} - \frac{V_S^2(R_{\max})}{V(R_{\max})R_{\max}^2} = \gamma \int_R^{R_{\max}} \left(\frac{1}{VR^2}\right)\left(V\frac{\partial V}{\partial R} + \frac{GM_\odot}{R^2}\right) \mathrm{d}R \,. \tag{9}$$

The second term on the left-hand side of the equation is the constant of integration. One may integrate Equation (9) by taking as $V(R)$ the corresponding dependence for the main quasi-stationary SW in the ray in Figure 3 (solid curve) and putting const $= 0$. (This choice of value for the constant of integration will be substantiated below). The dependence $V_S(R)$ that is obtained as a result of the integration within ≈ 1.7–$15.0\ R_\odot$, is presented in Figure 5 (solid line). The main plasma flow is found to exceed the sound velocity $V \approx V_S \approx 112$ km s^{-1} at $R \approx 7\ R_\odot$. The relative error may be estimated from

$$z = \left(\frac{V_S(R_{\max})R}{V_S(R)R_{\max}}\right)^2 \left(\frac{V(R)}{V(R_{\max}}\right) \,, \tag{10}$$

which is allowed for at $R \approx 7\ R_\odot$ since the constant of integration is set to zero (see above). We take (according to Figures 3 and 5): $V = 112$ km s^{-1} at $R = 7\ R_\odot$, $V = 175$ km s^{-1} at $R = R_{\max} = 15\ R_\odot$, and $V_S(R_{\max})/V_S(R) < 1$, and get $z < 14\%$. As the Sun is approached, the error of the calculated sound velocity decreases rapidly to $z < 2\%$ already at $R = 4\ R_\odot$.

The plasma temperature $T(R) = [T_e(R) + T_p(R)]/2$, calculated from $V_S(R)$, is plotted in Figure 6 by a solid line. Besides, crosses in Figure 6 show the portion of the experimental dependence of the electron temperature $T_e(R)$ according to recent measurements from SOHO (David *et al.*, 1997), and dark circles correspond to the estimated values of the temperature T from formula (1) for the broadening (with the distance) forefront δ of a high-density plasma flow travelling within a less dense plasma along the ray.

Observational data and results from two independent methods for estimating the temperatures T in Figure 6 lead us to conclude that in the streamer belt at $R < 6\ R_\odot$:

(1) At $R < 1.5\ R_\odot$, we have $T \approx T_e \approx T_p$, i.e., the proton and electron temperatures do not differ much, and they do not exceed 1.2–1.3×10^6 K.

(2) The temperature T decreases with the distance, and at $R \approx 5\ R_\odot$ one has $T < 5 \times 10^5$ K.

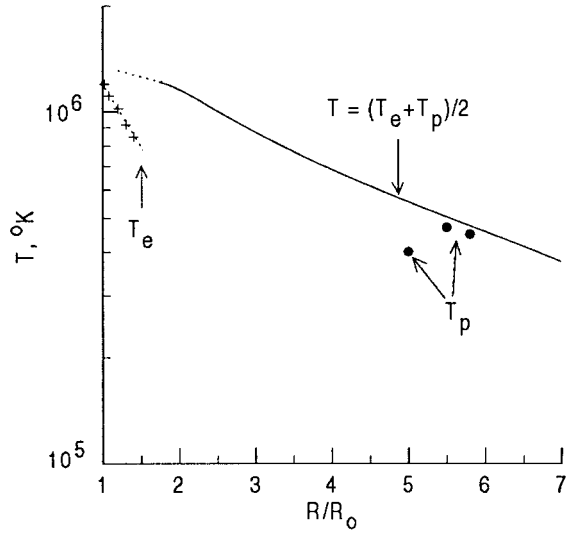

Figure 6. Distributions in the streamer belt: *solid line* – calculated temperature $T(R) = [T_e(R) + T_p(R)]/2$; • – calculated by formula (1); + – measured electron temperature $T_e(R)$ from David *et al.* (1997).

5. Conclusions

(1) It has been shown that the main quasi-stationary solar wind (SW), with a typical lifetime of up to 10 days, flows along the rays of the streamer belt. Depending on R, the velocity increases gradually from $V \approx 3$ km s^{-1} at $R \approx 1.3\ R_\odot$ to $V \approx 175$ km s^{-1} at $R \approx 15\ R_\odot$.

(2) We have studied the flows in the main solar wind forefront during the stage when it occupies the ray, i.e., at the stage of formation of a quasi-stationary plasma flow in the ray. It has been shown that the front width of the main SW increases almost linearly with its distance from the Sun.

(3) The initial velocity of the 'blob' increases with the distance from the Sun, where it originated, and is similar to the velocity of the main solar wind which carries it away. The typical width of the 'blob's' front $\delta \approx R_\odot$, which remains almost unchanged as the 'blob' moves away from the Sun.

(4) It is found that the main SW in the brightest rays of the streamer belt, at least within distances of the order of $R \approx 3\ R_\odot$, represents a flow of collisional magnetized plasma along the magnetic field. Near the Sun, at $R \leq 1.5\ R_\odot$, the half-sum of electron and proton temperatures does not exceed the values of $T = 1.5 \times 10^6$ K and decreases with distance from the Sun to $T < 5 \times 10^5$ K at $R \approx 5\ R_\odot$.

Acknowledgements

The SOHO/LASCO data used here are produced by a consortium of the Naval Research Laboratory (U.S.A.), Max-Planck-Institute für Aeronomie (Germany), Laboratoire d'Astronomie (France), and the University of Birmingham (U.K.). SOHO is a project of international cooperation between ESA and NASA.

We are grateful to V. G. Mikhalkovsky for his assistance in preparing the English version of the manuscript.

Grant governmental support for Russian Federation's leading scientific schools N001596659 and GNTP 'Astronomy'.

References

Artsimovich, L. A.: 1961, *Controlled Thermonuclear Reactions*, State Publishing House of Phys. and Math. Literature, Moscow, p. 54.

David, C. *et al.*: 1997, *The Corona and Solar Wind near Minimum Activity*, Oslo, Norway, 17–20 June 1997, p. 319.

Dollfus, A. and Martres, M.-J.: 1977, *Solar Phys.* **53**, 449.

Eselevich, V. G. and Eselevich, M. V.: 1999, *Solar Phys.* **188**, 299 (Paper I).

Eselevich, V. G. and Eselevich, M. V.: 2000, *Solar Phys.* **197** (in press).

Hundhausen, A. J.: 1993, *J. Geophys. Res.* **98**, 13177.

Sheeley, Jr. N. R. *et al.*: 1997, *Astrophys. J.* **485**, 472.

Wang Y.-M. *et al.*: 1998, *Astrophys. J.* **498**, L165.

Wang Y.-M. *et al.*: 1999a, *Geophys. Res.* **26**, 1203.

Wang Y.-M. *et al.*: 1999b, *Geophys. Res.* **26**, 1349.

Zeldovich, Ya. B. and Raizer, Yu. P.: 1966, *The Physics of Shock Waves and High-Temperature Hydrodynamic Phenomena*, Nauka, Moscow, p. 43.